Hindawi
Geofluids
Volume 2019, Article ID 3525818, 12 pages
https://doi.org/10.1155/2019/3525818

Research Article

An Improved Scheme of Frequency-Dependent AVO Inversion Method and Its Application for Tight Gas Reservoirs

Jiong Liu,[1,2,3] **Jun-rui Ning**,[1,2,3] **Xi-wu Liu**,[1,2,3] **Chun-yuan Liu**,[1,2,3] **and Tian-sheng Chen**[1,2,3]

[1]*National Key Laboratory of Corporation of Shale Oil/Gas Enrichment Mechanism and Effective Development, China*
[2]*Sinopec Key Laboratory of Shale Oil/Gas Exploration and Production Technology, China*
[3]*Sinopec Petroleum Exploration and Production Research Institute, China*

Correspondence should be addressed to Jiong Liu; jiong3330@aliyun.com

Received 19 June 2018; Revised 30 October 2018; Accepted 14 November 2018; Published 3 February 2019

Academic Editor: Umberta Tinivella

AVO inversion is a seismic exploration methodology used to predict the earth's elastic parameters and thus rocks and fluid properties. It is built up on elastic theory and does not consider the seismic dispersion in real strata. Recent experiments and theory of rock physics have shown that in hydrocarbon-bearing rocks, especially in gas-bearing ones, the change of seismic velocity with frequency may be pretty remarkable for fluid flow in pore space. Some scholars proposed methods about seismic dispersion, such as frequency-dependent AVO inversion, to forecast oil and gas reservoirs underground. In this paper, we demonstrate an improved scheme of frequency-dependent AVO inversion, which is based on conventional Smith-Gidlow's AVO equation, to extract seismic dispersion and predict the hydrocarbon underground. A simple model with gas-bearing reservoir is devised to validate the inversion scheme, and further analysis indicates that our scheme is more accurate and reasonable than the previous scheme. Our new scheme applied to the tight gas reservoirs in Fenggu area of western Sichuan depression of China finds that regions with high dispersion gradients correlate well with regions with prolific gas. Analysis and case studies show that our scheme of frequency-dependent AVO inversion is an efficient approach to predict gas reservoirs underground.

1. Introduction

The amplitude versus offset (AVO) is one of the most widely used geophysical techniques to predict oil and gas reservoirs [1]. Since Ostrander [2] developed the AVO technique to identify "bright spot" reservoirs, many scholars have studied AVO extensively and got many successful cases [3–9].

AVO approaches mentioned above are based on the assumption that subsurface rocks are elastic. However, recent developments in seismic rock physics theory and practical studies have revealed that underground strata are viscoelastic, and seismic wave always has noticeable dispersion and attenuation for fluid flow in pore space of rocks [10–16]. However, the dispersion characteristics of seismic wave in the actual medium are not considered in the conventional AVO techniques.

In rocks bearing oil, gas, or water, the seismic velocity is dependent on frequency. Especially in those bearing abundant gas, there may be remarkable seismic dispersion. The more fluid the rocks hold, the greater the seismic wave disperses at seismic frequency band. Therefore, seismic velocity dispersion may be used to identify the fluid in porous rocks underground. This has attracted some researchers to study and apply dispersion in hydrocarbon exploration. Chapman et al. [17] studied the dispersion effects on the variance of AVO based on a porous medium model and verified the potential of seismic dispersion for the detection of oil and gas reservoirs. Wilson et al. [18] proposed a frequency-dependent method to extract dispersion information from prestack seismic data and predicted the gas reservoirs in North Sea. Wu et al. [19] presented a new technique of spectrum decomposition to improve the accuracy of Wilson's method. Some successful cases have been reported by frequency-dependent AVO analysis [20–23]. These researches show that seismic dispersion may be a tool to predict hydrocarbon reservoirs underground. However,

there is an imperfection in Wilson's scheme of frequency-dependent inversion because it cannot give a reasonable explanation for the high S-wave dispersion in its results.

In this paper, we develop an improved scheme of frequency-dependent AVO inversion to predict tight gas reservoirs. Analysis and case studies show that the new frequency-dependent AVO inversion scheme is more reasonable and accurate than the previous scheme.

2. Frequency-Dependent AVO Inversion

In this part, Wilson's scheme of frequency-dependent AVO is briefly introduced first. Then, our improved scheme is derived in detail and analytical comparison between two schemes is made. Finally, a signal decomposition technique, which is used to obtain seismic records at different frequencies in frequency-dependent AVO inversion, is illustrated.

2.1. Wilson's Scheme. AVO inversion is a seismic exploration methodology used to predict the earth's elastic parameters and thus rocks and fluid properties. Zoeppritz derived the formulations of reflectivity and transmissivity when a plane wave impinges on an interface of different strata underground and developed the theoretical work for AVO theory. Assuming the difference of elastic parameters across an interface is small, Aki and Richards [24] derived an approximation equation of reflectivity. Smith and Gidlow substituted the Gardner's relation between density and P-wave's velocity into Aki-Richard's equation and obtained the following AVO equation named Smith-Gidlow's equation [25]:

$$R(\theta) \approx \frac{5}{8}\frac{\Delta V_p}{V_p} - \frac{V_s^2}{V_p^2}\left(4\frac{\Delta V_s}{V_s} + \frac{1}{2}\frac{\Delta V_p}{V_p}\right)\sin^2\theta + \frac{1}{2}\frac{\Delta V_p}{V_p}\tan^2\theta, \tag{1}$$

where R is P-wave's reflectivity, V_p and V_s are the average of P- and S-wave velocities of strata on both sides of the interface, θ is the incident angle, and ΔV_p and ΔV_s are, respectively, P- and S-wave velocity difference between the adjoining medium.

The Smith-Gidlow's equation has been widely used in geophysics. But it is based on elasticity, and it does not consider the seismic dispersion in real rocks.

Considering the seismic velocity is dependent on frequency in rocks, Wilson et al. [18] extended the Smith-Gidlow's equation into frequency domain and derived a frequency-dependent AVO equation. The equation's expression is

$$R(\theta, f) \approx A(\theta)\frac{\Delta V_p}{V_p}(f_0) + (f - f_0)A(\theta)I_a + B(\theta)\frac{\Delta V_s}{V_s}(f_0) + (f - f_0)B(\theta)I_b, \tag{2}$$

where f denotes frequency and f_0 is reference frequency. Coefficients $A(\theta)$ and $B(\theta)$ are

$$A(\theta) = \frac{5}{8} - \frac{1}{2}\frac{V_s^2}{V_p^2}\sin^2\theta + \frac{1}{2}\tan^2\theta, \tag{3}$$

$$B(\theta) = -4\frac{V_s^2}{V_p^2}\sin^2\theta. \tag{4}$$

In equation (2), I_a and I_b are called P- and S-wave dispersion gradients and their expressions are

$$I_a = \frac{d}{df}\left(\frac{\Delta V_p}{V_p}\right)\Bigg|_{f=f_0}, \tag{5}$$

$$I_b = \frac{d}{df}\left(\frac{\Delta V_s}{V_s}\right)\Bigg|_{f=f_0}. \tag{6}$$

I_a and I_b denote the dispersion magnitude of the P- and S-wave at the reference frequency f_0. In rocks bearing oil, gas, and water, the seismic velocity is dependent on frequency. Especially in rocks bearing abundant gas, there may be remarkable seismic dispersion. Therefore, I_a and I_b can be regarded as attributes to predict the fluids underground.

2.2. An Improved Scheme. Although some cases of success have been reported by Wilson's frequency-dependent AVO inversion, there are some problems in the equation. The item V_s^2/V_p^2 is assumed to be independent of frequency during the derivation of equation (2). The assumption contradicts the premise that seismic velocities are frequency dependent.

In this paper, we derive an improved scheme of frequency-dependent AVO inversion without the unreasonable assumption in Wilson's scheme. The following is the derivation process of the improved one.

First, the Smith-Gidlow's equation (1) can be recast into

$$R(\theta) = A_1(\theta)\frac{\Delta V_p}{V_p} + B_1(\theta)\left[\frac{V_s^2}{V_p^2}\left(\frac{\Delta V_s}{V_s} + \frac{1}{8}\frac{\Delta V_p}{V_p}\right)\right], \tag{7}$$

where

$$A_1(\theta) = \frac{5}{8} + \frac{1}{2}\tan^2\theta, \tag{8}$$

$$B_1(\theta) = -4\sin^2\theta. \tag{9}$$

Generally P-wave reflection coefficient R, P-, S-wave velocities and the ratio V_s^2/V_p^2 are frequency-dependent in real strata. So, equation (7) can be extended into frequency domain, whose expression is

$$R(\theta, f) = A_1(\theta)\frac{\Delta V_p}{V_p}\Bigg|_f + B_1(\theta)\left[\frac{V_s^2}{V_p^2}\left(\frac{\Delta V_s}{V_s} + \frac{1}{8}\frac{\Delta V_p}{V_p}\right)\right]\Bigg|_f. \tag{10}$$

Expanding equation (10) at a reference frequency f_0 by Taylor series, neglecting second and higher order items of $f - f_0$, we then get the reflection coefficient of P-wave in the frequency domain

$$R(\theta, f) = A_1(\theta)\frac{\Delta V_p}{V_p}\bigg|_{f_0} + B_1(\theta)\left[\frac{V_s^2}{V_p^2}\left(\frac{\Delta V_s}{V_s} + \frac{1}{8}\frac{\Delta V_p}{V_p}\right)\right]\bigg|_{f_0} + (f - f_0)A_1(\theta)I_{a1} + (f - f_0)B_1(\theta)I_{b1}, \tag{11}$$

where I_{a1} and I_{b1} are

$$I_{a1} = \frac{d}{df}\left(\frac{\Delta V_p}{V_p}\right)\bigg|_{f=f_0}, \tag{12}$$

$$I_{b1} = \frac{d}{df}\left[\frac{V_s^2}{V_p^2}\left(\frac{\Delta V_s}{V_s} + \frac{1}{8}\frac{\Delta V_p}{V_p}\right)\right]\bigg|_{f=f_0}. \tag{13}$$

Because there is a relationship as

$$R(\theta, f_0) = A_1(\theta)\frac{\Delta V_p}{V_p}\bigg|_{f_0} + B_1(\theta)\left[\frac{V_s^2}{V_p^2}\left(\frac{\Delta V_s}{V_s} + \frac{1}{8}\frac{\Delta V_p}{V_p}\right)\right]\bigg|_{f_0}, \tag{14}$$

equation (11) can finally be simplified as

$$R(\theta, f) - R(\theta, f_0) = (f - f_0)A_1(\theta)I_{a1} + (f - f_0)B_1(\theta)I_{b1}. \tag{15}$$

Equation (15) is our frequency-dependent AVO inversion equation in this paper.

From the equation of (12), we can see that I_{a1} denotes the velocity derivative versus frequency of P-wave and we call it P-wave dispersion gradient. Since seismic dispersion in gas reservoirs always is strong, I_{a1} can be used as a tool to detect the "sweet spots" of gas reservoirs. On the other hand, I_{b1} represents the derivatives of mixing P- and S-wave versus frequency, which we call mixed dispersion gradient. It is more complicated than I_{a1}. Since the underlying physical mechanism of S-wave's dispersion in fluid-bearing rocks is unclear presently, only P-wave's dispersion gradient I_{a1} is used to predict the gas reservoirs and I_{b1} is ignored in the rest of the paper.

It is should be noted that there is reference frequency f_0 in the formulation (10). The choosing of f_0 always determines the results of frequency-dependent AVO inversion. If f_0 is located in the domain where seismic dispersion is not remarkable, the inversion results may be suppressed by noise, and the results will deteriorate. We choose the dominant frequency of seismic wavelet as f_0 because the dispersion at the vicinity of dominant frequency usually is obvious in real data.

Our scheme of frequency-dependent AVO inversion is inspired by Wilson's scheme, but it is improved. First, there is no unreasonable assumption that V_s^2/V_p^2 is frequency independent in Wilson's scheme. So our scheme is more accurate in theory. Second, V_s^2/V_p^2 is included in the unknown term I_{b1} in the new scheme and does not need estimating before inversion. While V_s^2/V_p^2 is included in the inversion matrix in Wilson's scheme, and it needs estimating. So our scheme is more convenient than Wilson's.

2.3. Smoothed Pseudo Wigner-Ville Distribution. Obtaining seismic records at different frequencies is an important step of frequency-dependent AVO inversion. Many methods can decompose seismic data into parts in different frequency bands, such as Fourier transform, short-time Fourier transform (STFT) and wavelet transform etc. Here, a signal decomposition technique named smoothed pseudo Wigner-Ville distribution (SPWVD) is introduced. The comparison between SPWVD and other methods, such as STFT and wavelet transform, is also made to test the accuracy of SPWVD.

Wigner-Ville distribution (WVD) is one of the most effective approaches to decompose nonstationary signal on the time-frequency plane via an energy distribution function. The time-frequency decomposition of a signal $x(t)$ by WVD is expressed as [26]

$$\mathrm{WVD}(t, f) = \int_{-\infty}^{\infty} X\left(t + \frac{\tau}{2}\right)\bar{X}\left(t - \frac{\tau}{2}\right)e^{-j2\pi f\tau}d\tau, \tag{16}$$

where τ is the time delay and $X(t)$ is the analytic signal corresponding to $x(t)$. Different from short-time Fourier transform, WVD does not have a window function and avoids the contradiction that the time resolution and frequency resolution mutually constrain during STFT. However, as defined in equation (16), WVD is not linear, which means the WVD of two signals' sum is not equal to the sum of each signal's WVD because of a cross term in the WVD sum. These cross terms generate a false energy distribution which is one of most important issues when WVD is used for time-frequency analysis of multicomponent nonstationary signal. To mitigate the impact of cross terms, modified approaches called smoothed pseudo Wigner-Ville distribution (SPWVD) have been proposed, and it is defined as [26]:

$$\mathrm{SW}_{g,h,X} = \int_{-\infty}^{+\infty}\int_{-\infty}^{+\infty} X\left(t + \frac{\tau}{2}\right)\bar{X}\left(t - \frac{\tau}{2}\right)g(\nu)h(\tau)e^{-j2\pi f\tau}d\nu d\tau, \tag{17}$$

where ν is time delay, and τ is frequency offset. $g(\nu)$ is the time smoothing window while $h(\tau)$ is the frequency smoothing window. If both $g(\nu)$ and $h(\tau)$ are real symmetric

functions, $g(0) = h(0)$. The selections of two smoothing windows are independent of each other. It is possible to attenuate the cross terms in WVD by the two smoothing windows. For example, the two smoothing windows $h(\tau)$ and $g(\nu)$ could both be Gaussian functions.

$$\phi(\nu, \tau) = g(\nu)h(\tau) = e^{-\alpha\nu^2-\beta\tau^2} \quad \alpha \geq 0,\ \beta \geq 0, \tag{18}$$

in which $\phi(\nu, \tau)$ is the smoothing function in time-frequency space and α and β are coefficients designed to adjust the bandwidth of the Gaussian functions.

For a synthetic or a seismic trace, the magnitudes of decomposed components at different frequencies are different for two factors. One is different reflection coefficients at different frequencies, which is caused by dispersion. The other is the different magnitude of wavelet components. Frequency-dependent AVO inversion considers the reflection coefficients at different frequencies. So, the effects of the wavelet must be removed before frequency-dependent AVO inversion. An efficient spectrum balance technique [27] is adopted in this paper.

In the following frequency-dependent AVO inversion, the SPWVD technology is used to obtain seismic records at different frequencies.

2.4. Validation the Scheme of Frequency-Dependent AVO Inversion. In this part, a simple model with horizontal layers is devised to test our scheme of frequency-dependent AVO inversion. Comparison of results by Wilson's scheme and ours is also made for the model.

The simple model is composed by three horizontal layers as shown in Figure 1. The top two layers are nonreservoir and are regarded as elastic medium without dispersion. The bottom layer is gas-bearing reservoir with strong dispersion, and poroelastic medium is adopted to represent it. The parameters of each layer are shown in Table 1. Parameters V_p and V_s are P- and S-wave velocities, ρ is the density, and φ is the porous volume; S_w and S_g are water and gas saturation. For layer 1 and layer 2, there are no S_w or S_g because they are elastic medium.

Reflection coefficients at the interface between layer 1 and layer 2 can be computed easily by Aki-Richard's equation or Smith-Gidlow's equation. Then, corresponding synthetics can be obtained by convolution between the coefficients and wavelet. But the synthetics at the interface between layer 2 and layer 3 are more difficult to get because the seismic velocity is dependent on frequency. We first compute the seismic velocities at different frequencies on patchy model [28] and derive the corresponding reflection coefficients from seismic velocities. Then, the frequency components of the wavelet are computed by fast Fourier transform, and the components are multiplied with reflectivity at different frequencies. Finally, the results are transformed into time domain to get the synthetics by inverse fast Fourier transform. Because the patchy model of poroelasticity only considers the P-wave dispersion caused by porous fluid, the synthetics include the effects of P-wave dispersion and those of S-wave are not included. This characteristic will be used to test the rationality of frequency-dependent AVO inversion by Wilson's scheme and ours later.

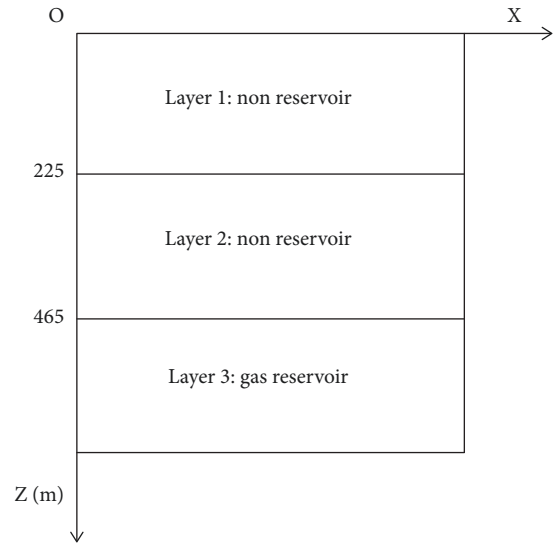

Figure 1: A horizontally layered medium model. The top two layers are nonreservoir and are regarded as elastic medium. The bottom layer is gas-bearing reservoir and poroelastic medium is adopted to represent it.

Table 1: The parameters of layered medium model.

	V_P (m/s)	V_S (m/s)	ρ (g/cm^3)	φ	S_w	S_g
Layer 1	4500	2700	2.4	—	—	—
Layer 2	4800	3200	2.6	—	—	—
Layer 3	3458	2100	2.3	0.08	0.4	0.6

Figure 2 shows the prestack synthetics at thirteen incidence angles 2°, 3° … 13°, which are computed by Ricker wavelet with 30 Hz dominant frequency. The peak at 0.1 s coincides with the interface across the top two nonreservoir layers and the trough at 0.2 s with the interface between the nonreservoir and gas-reservoir layers.

SPWVD technique is used to decompose the synthetics. Figure 3 shows the original decomposition (Figure 3(a)) and balanced (Figure 3(b)) results of the synthetic at frequencies 26 Hz, 28 Hz, 30 Hz, 32 Hz, and 34 Hz with 6° incidence angle. We can see that the effects of seismic wavelet are eliminated by spectrum balance technique. The remaining energy differences with various frequencies at 0.2 s are caused by seismic dispersion.

Figure 4 is the inversion results based on the new inversion scheme for the layered model. To compare our scheme with the previous one, the inversion by Wilson's scheme is made and also shown in Figure 4. From Figure 4(a), we can see the value of I_{a1}, the P-wave dispersion gradient of our results, is large at the interface between elastic and poroelastic medium, while the value at the elastic-elastic interface is rather small. The inversion result is consistent with the model condition that dispersion effects exist on the elastic-poroelastic interface

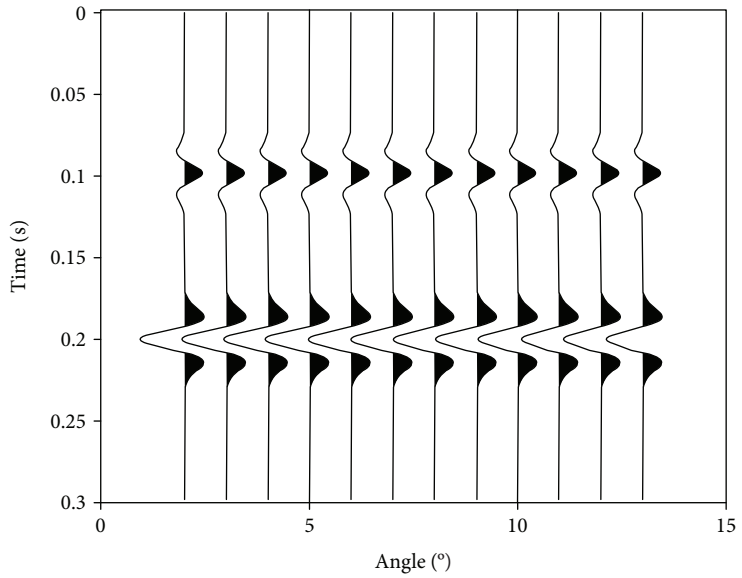

Figure 2: The prestacked synthetics at different incidence angles for layered medium model. The peak at 0.1 s coincides with the interface across the top two elastic nonreservoir layers. The trough at 0.2 s coincides with the interface between the elastic nonreservoir and poroelastic gas-reservoir layers.

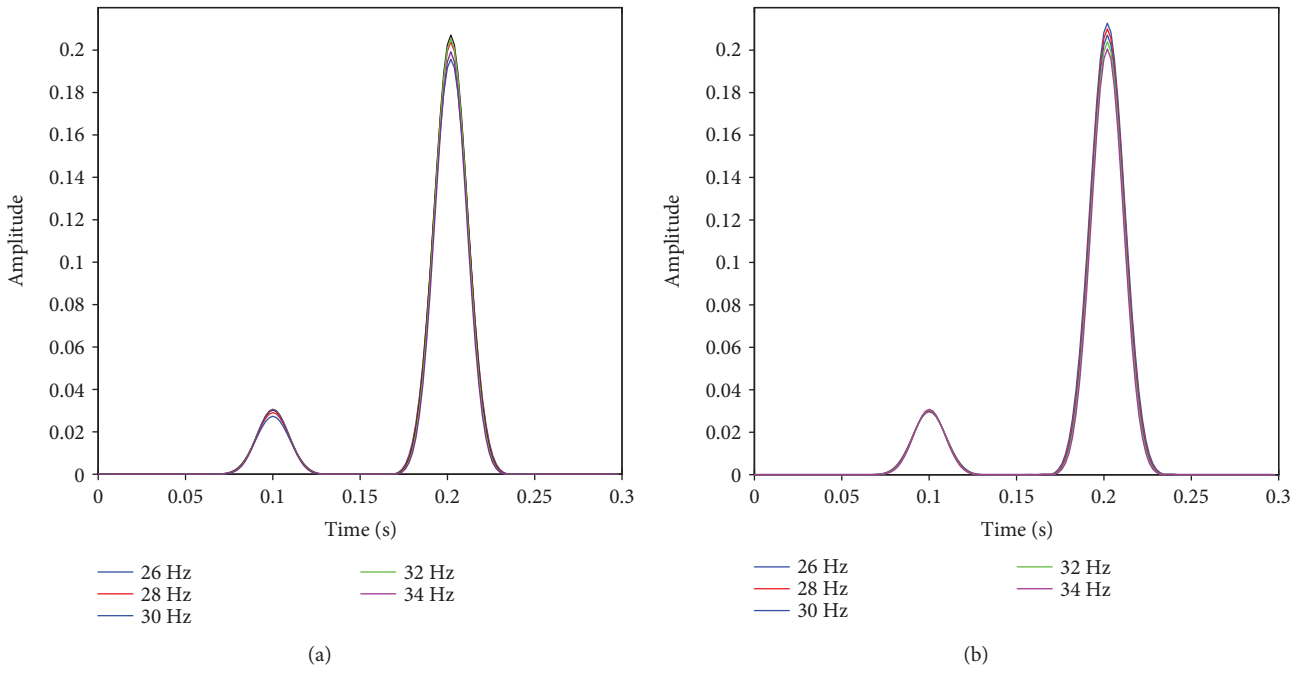

Figure 3: (a) Decomposed synthetic at 6° incidence for layered medium model by SPWVD. (b) The balanced results of the decomposed synthetic. The effects of seismic wavelet at different frequency are eliminated by spectrum balance technique. The remaining energy differences with various frequencies at 0.2 s are caused by seismic dispersion.

and do not exist on the elastic-elasticone. The model results also show that the P-wave dispersion gradient can be used to predict subsurface reservoirs and our frequency-dependent inversion scheme is workable. Similarly, the peak of inversion result I_a by Wilson's scheme matches the interface between elastic and poroelastic medium too. But the value is less than ours at the peak. In Figure 4(b), the mixed dispersion gradient I_{b1} of our results also matches the interface of elastic and poroelastic medium. The S-wave's dispersion gradient I_b of Wilson's scheme has similar character. However, the S-wave's dispersion gradient I_b should be zero because S-wave is set to be independent of frequency in the model. Obviously, the result of I_b is not reasonable. Through analysis, we think that is caused by unreasonable assumption that V_s^2/V_p^2 is frequency independent in equation (2). The inversion results show that Wilson's scheme is not reasonable

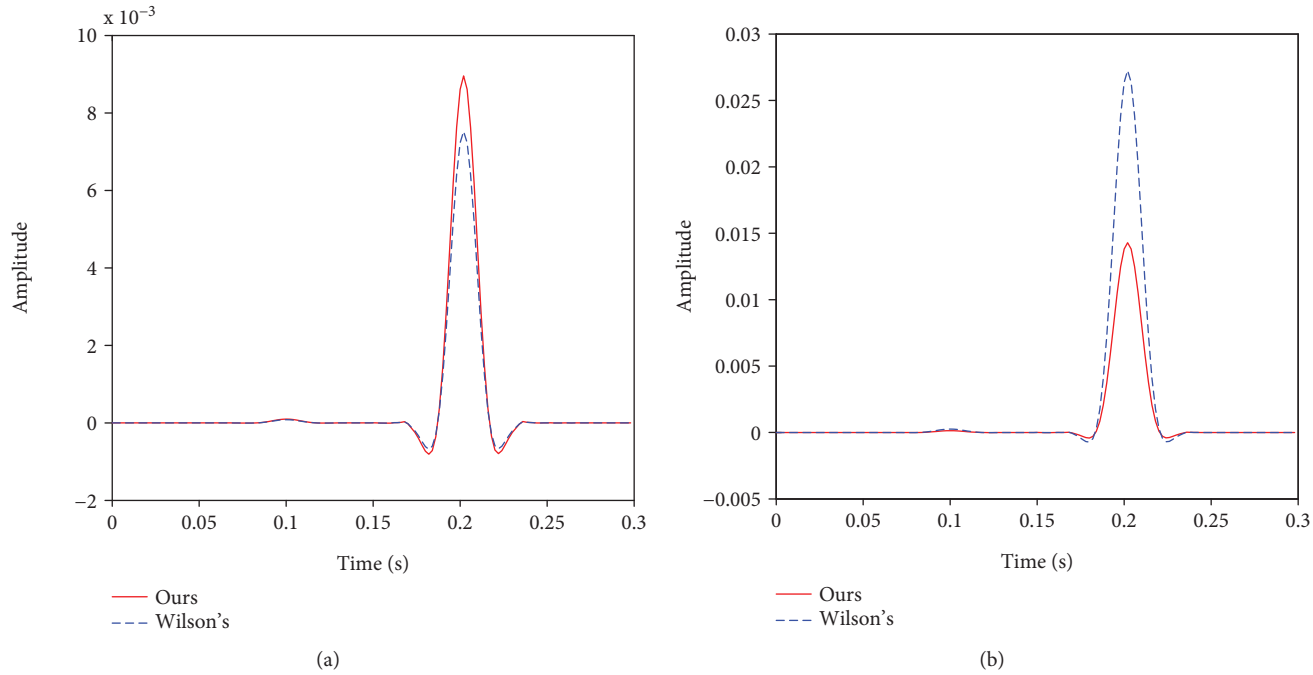

Figure 4: The inversion results by our scheme and Wilson's scheme. (a) P-wave dispersion gradients I_{a1} by our scheme and I_a by Wilson's. The value by Wilson's schemes is less than that by ours at the peak; (b) mixed dispersion gradient I_{b1} by our scheme and S-wave dispersion gradient I_b by Wilson's. The value of I_b is unreasonable.

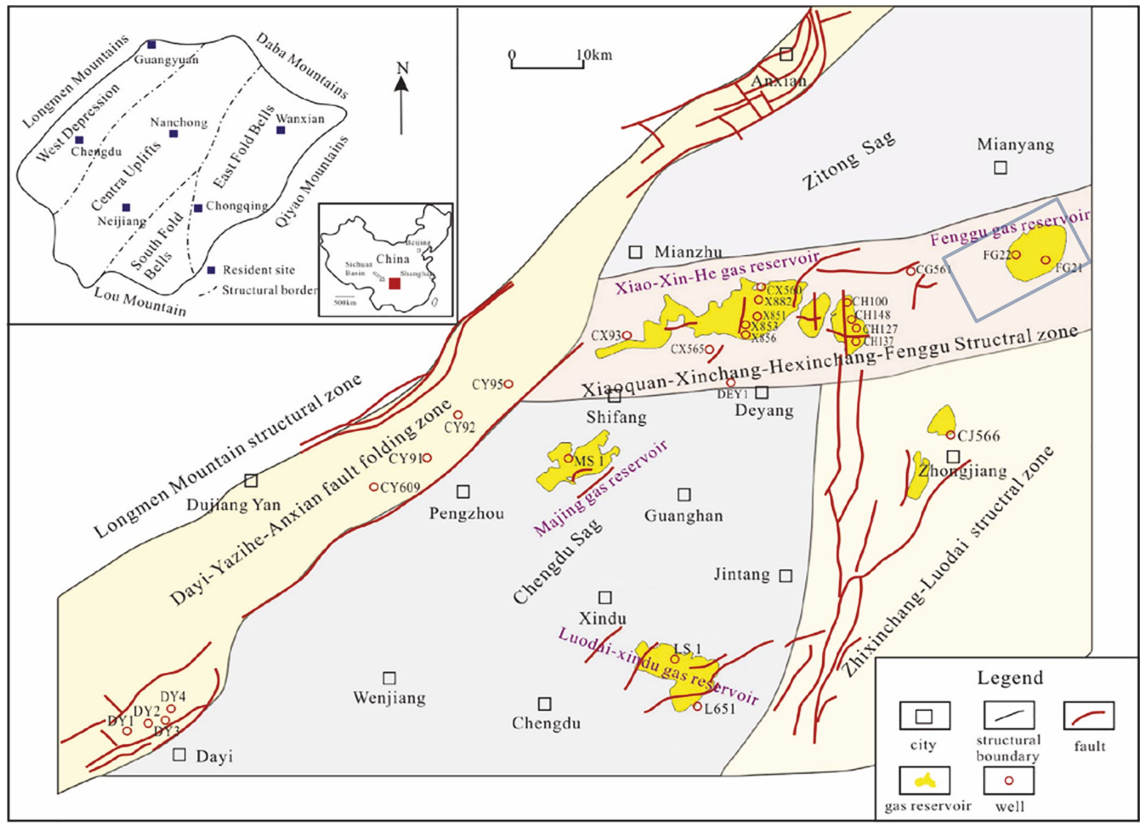

Figure 5: Location of Fenggu area and tectonic divisions of western Sichuan Basin [29]. The Fenggu structure is located in eastern end of the Xiaoquan-Hexingchang-Xinchang-Fenggu structural zone in western Sichuan depression, China. The area framed by blue rectangular is the objection area of the paper.

Stratum			Thickness (m)	Depth (m)	Lithology
System	Formation	Member			
Upper Triassic	Xujiahe (T_3x)	T_3x^5	470~550	2500~3500	
		T_3x^4	535~610	3100~4150	
		T_3x^3	720~770	3700~4700	
		T_3x^2	500~560	4500~5300	

Sandstone
Mudstone

Figure 6: Developing feature of strata in Xujiahe formation, Fenggu area [29]. In late Triassic, a thick set of sediment was deposited in Xujiahe formation with T_3x^2, T_3x^3, T_3x^4, and T_3x^5 members positioned from bottom to top in Fenggu area.

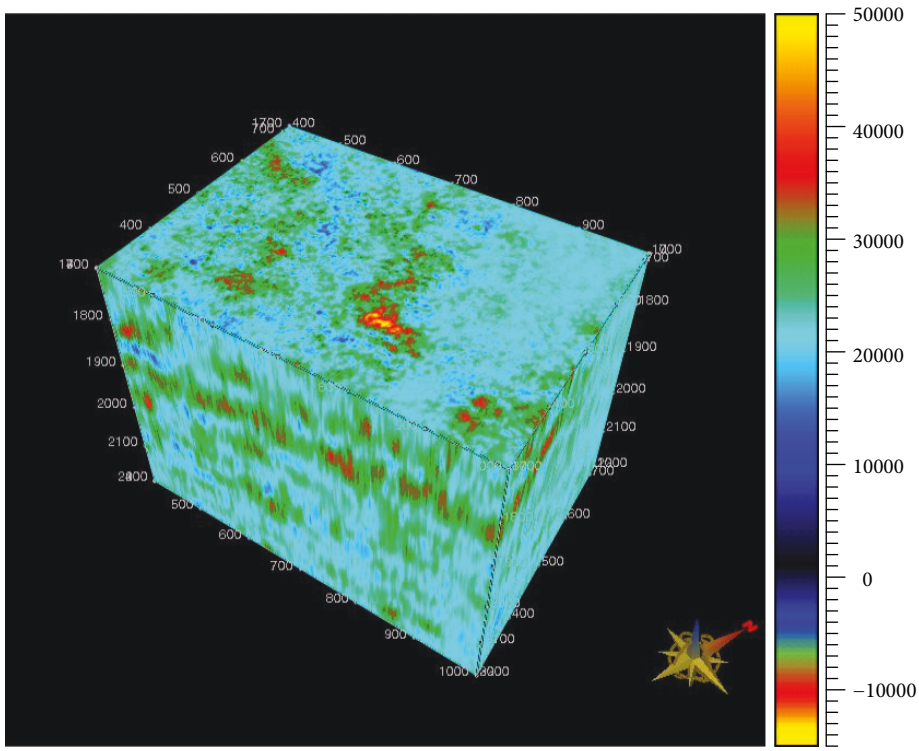

Figure 7: P-wave dispersion gradient of T_3x^4 member in the Xujiahe formation, Fenggu area. The color bar represents the amplitude of P-wave dispersion gradient.

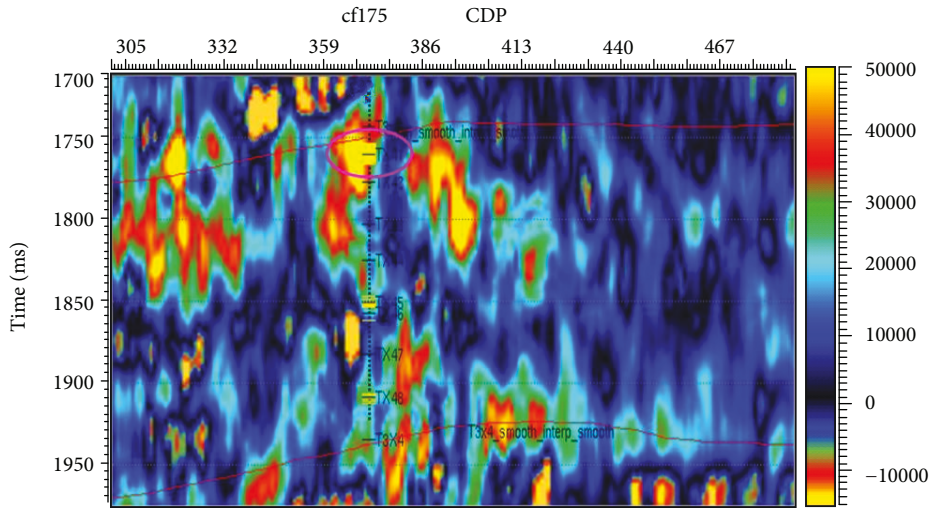

Figure 8: The inversion profile through well cf175. The region marked by the purple ellipse is a good conventional gas reservoir. It has big value of P-wave dispersion gradient. Our inversion results match the well tests in this domain.

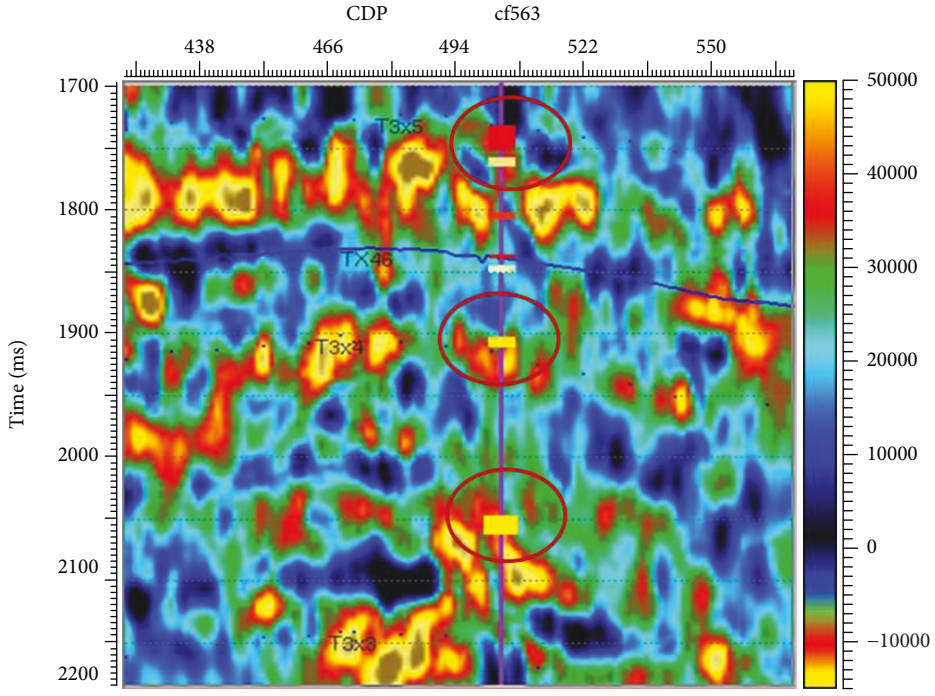

Figure 9: The inversion profile through well cf563. The three domains marked by ellipses are fractured or conventional gas reservoirs. These regions have big value of P-wave dispersion gradient. The inversion results match the well tests in these domains.

for S-wave dispersion gradient. On the contrary, the nonzero value of I_{b1} at the elastic-elastic interface in our results can be interpreted reasonably by the term of $V_s^2/V_p^2((\Delta V_s/V_s) + (1/8)(\Delta V_p/V_p))$ because P-wave is frequency dependent. Our scheme is more reasonable than Wilson's.

Since the mixed dispersion gradient has similar characters with that of P-wave dispersion gradient, in following application, we only employ P-wave dispersion gradient I_{a1} to detect gas reservoirs underground.

3. The Application of Frequency-Dependent AVO Inversion

In this part, we first introduce the geology background of Fenggu area briefly. Then, our scheme of frequency-dependent AVO inversion is applied to predict the gas reservoirs in this area.

3.1. Geology Background. The Fenggu structure is located in eastern end of the Xiaoquan-Hexingchang-Xinchang--Fenggu structural zone in western Sichuan depression, China

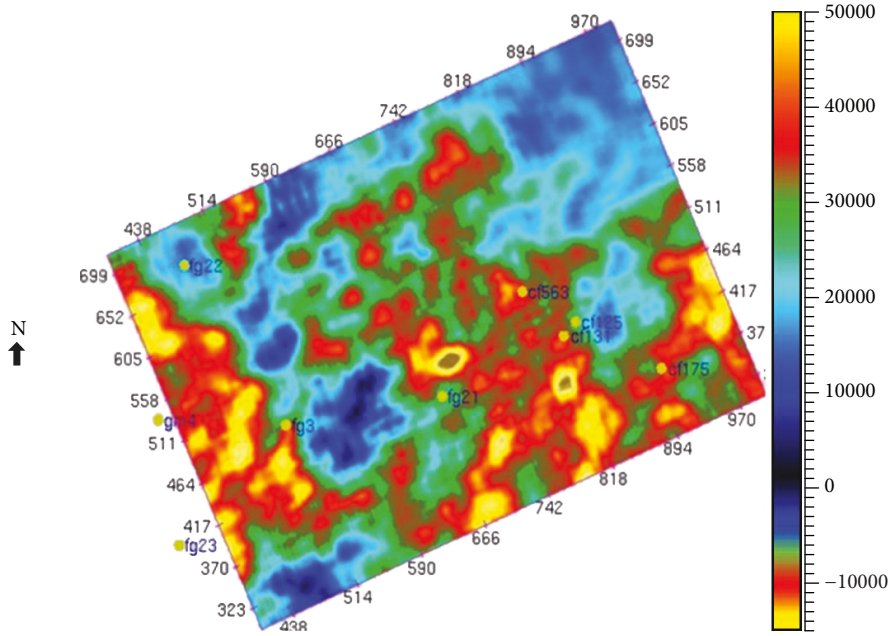

Figure 10: Time–slice of P-wave dispersion gradient along the first set sand of T_3x^4 member. Inversion results show that the west and the southeast of the area is the favorable zone of gas reservoirs for the high value of P-wave dispersion gradient.

Table 2: Logging results of the first set sand of T_3x^4 member.

	Fg22	Cf175	Cf125	Cf563	Fg21
Test result	Mudstone	Poor gas reservoir	Poor gas reservoir	Gas reservoir	Poor gas reservoir

(Figure 5). In late Triassic, a thick set of sediment was deposited in Xujiahe formation. T_3x^2, T_3x^3, T_3x^4, and T_3x^5 members are positioned from bottom to top in Xujiahe formation (Figure 6), with T_3x^1 member absent but developed in other parts of western Sichuan depression. Geology studies show that the gas source in Xujiahe formation of Fenggu area is mega.

In Upper Triassic Xujiahe formation, Fenggu area, T_3x^4 member is considered highly prospective for gas. The favorable sedimentary include plain river, frontal mouth bar of fan deltas, and meandering stream deltas facies. Rock physics tests show that reservoir porosity is primarily composed of secondary corrosion pores, remaining intergranular pores and developed micro fracturing. Since the average porosity and permeability are low, the reservoirs in T_3x^4 member of Xujiahe formation are tight gas reservoirs. In the following, we will detect gas reservoirs in T_3x^4 member.

3.2. Frequency-Dependent AVO Inversion in Fenggu Area. The scheme (15) of frequency-dependent AVO inversion is applied to 3D seismic data of T_3x^4 member, Xujiahe formation, Fenggu area. First prestack angle gathers are extracted from prestack seismic recordings (offset gathers) by seismic velocity. Subsequently, the SPWVD technique is used to derive angle gathers at different frequencies from prestack angle gathers. Next, the scheme (15) is applied on the angle gathers at different frequencies for inversion, and the dispersion gradient of P-wave is computed. Since the places with large P-wave dispersion gradient always correspond with hydrocarbon reservoirs, the gas reservoirs underground are predicted by the P-wave dispersion gradient.

Figure 7 shows the P-wave dispersion gradient cube of T_3x^4 member in the Xujiahe formation, Fenggu area. The color bar represents the amplitude of P-wave dispersion gradient.

Figure 8 is the inversion profile of P-wave dispersion along a seismic line through well cf175. The two red curves denote the top and bottom of T_3x^4 member. Colored blocks on well-path indicate logging fluid interpretation results, in which yellow one represents high-quality gas-bearing reservoir while the thickness of the color blocks denotes the abundance level of reservoirs. Inversion results indicate that there is a region with high value of P-wave dispersion gradient at well cf175 (marked by the purple ellipse), which means it may be a reservoir with gas. The test of well cf175 proves it is a good conventional gas reservoir. Our inversion results match the well tests in this region.

Figure 9 is another inversion profile through well cf563. Red blocks on well-path represent fractured gas reservoirs. Our inversion shows that the three domains marked by red ellipses may have abundant gas because of their high value of P-wave dispersion gradient. The well tests prove the regions are fractured or conventional gas reservoirs. Our inversions do match the well tests.

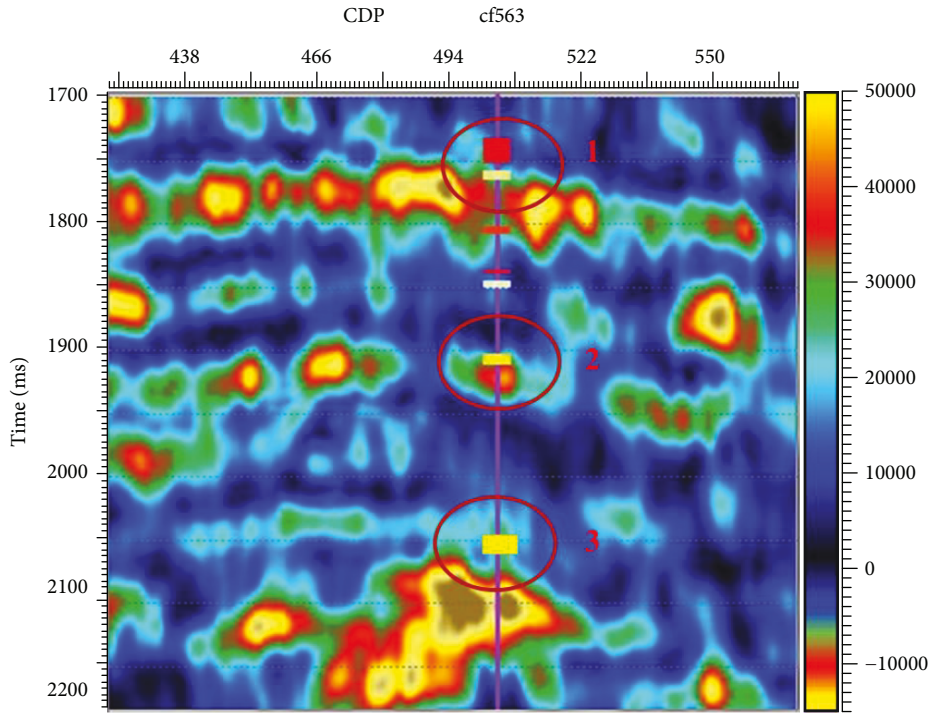

Figure 11: The inversion profile through well cf563 by Wilson's scheme. The prediction by Wilson's scheme matches the well test at location 2. But at the locations 1 and 3, the values of P-wave dispersion gradient are not high while they are good conventional and fractured gas reservoirs. The predictions by Wilson's scheme mismatch with well tests at the two locations.

Figure 10 is the slice of P–wave's dispersion gradient along the first set sand which is near the bottom of T_3x^4 member. Inversion results show that the west and the south-east of the area is the favorable zone of gas reservoirs for the high value of P-wave dispersion gradient.

In the object area, five wells reaching the bottom of T_3x^4 member have been drilled, and Table 2 shows the logging results of the first set sand of T_3x^4 member.

Comparison of P–wave's dispersion and the well tests in Table 1 reveals the following: the P-wave dispersion gradient value at cf563 is large and logging indicates the presence of a prolific gas reservoir; the P-wave dispersion gradient value is small at Fg22 and logging of this well shows that this area constitutes with mudstones; and inversion values at cf125 an cf21 are moderate and loggings indicate these regions are poor-quality gas reservoirs. It should be noted that region at well Cf175 is near the domain with large P-wave dispersion gradient but the inversion value is not large. It can be seen more clearly from Figure 9 that the region near the bottom of T_3x^4 at well cf175 has moderate P-wave dispersion gradient. Our predictions at well cf175 still match with the well tests. The comparison indicates that our predictions are right and the frequency-dependent AVO inversion by our scheme can be used to detect tight gas reservoirs underground.

3.3. Comparison of Frequency-Dependent AVO Inversions by Different Schemes. Frequency-dependent AVO inversion by Wilson's scheme is also done on seismic data of Fenggu area. Figure 11 is the inversion profile through well cf563. At location 2, the value of P-wave dispersion gradient is high and the prediction matches the well test. But at locations 1 and 3, the values of P-wave dispersion gradient are not high while well tests demonstrate the two places are good conventional and fractured gas reservoirs. The predictions by Wilson's scheme mismatch with well tests at the two locations. However, the predictions by our scheme (Figure 9) match well tests. The comparison for this profile shows that our scheme is more accurate than Wilson's.

Figure 12 is the inversion profile through well cf125 by the new scheme (Figure 12(a)) and Wilson's (Figure 12(b)). P–wave's dispersion gradients of the domain marked by red ellipse, which is near the bottom of T_3x^4 member, are low, and well test demonstrates the place is a poor gas reservoir (white block). Two inversion results match well test. However, comparison shows that result by our scheme has better continuity and more contrast than that by Wilson's.

4. Discussion and Conclusions

Dispersion is related to porous fluid when seismic wave propagates in reservoirs. In regions where porous fluid is abundant, the seismic dispersion is always great at seismic frequency band, especially in gas reservoirs. Frequency-dependent AVO inversion is indeed a method to extract P-wave dispersion gradient from prestack angle gathers. Further prediction of oil and gas reservoirs can be made by inverted dispersion gradient.

In this paper, we derived a scheme of frequency-dependent AVO inversion. It is motivated by Wilson's scheme, but is improved. The comparison between inversion results for a layered model by two different schemes shows that our scheme is more reasonable. Further practical

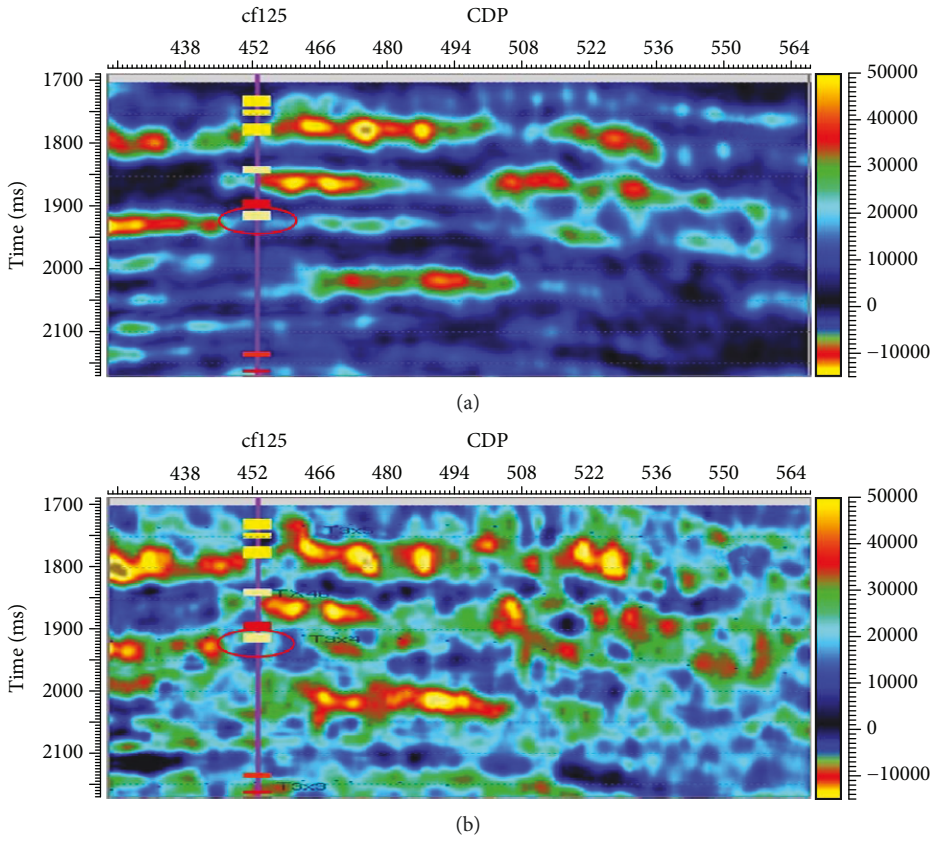

Figure 12: Inversion profile through well cf125 by the new scheme (a) and Wilson's (b). Two P–wave's dispersion gradients at the location marked by red ellipse are low, and well test indicates the place is a poor gas reservoir (white block). Two inversion results match well test. But comparison shows that result by our scheme has better continuity and more contrast than that by Wilson's.

application in Fenggu area is made on our inversion scheme. The predictions of gas reservoirs by our scheme of frequency-dependent AVO inversion match well tests. That verifies the effectiveness of our inversion scheme in prediction of gas reservoirs.

There is a point to be noted that the Gardner's equation about density and P-wave velocity is employed in the derivation of our inversion scheme. Since it is just an empirical equation, it may need modification for special regions, and the scheme of frequency-dependent AVO needs corresponding modification too. By this treatment, better inversion results can be expected. This task will be undertaken in our future work.

Data Availability

All model data during this study are listed in this manuscript; researchers can replicate the analysis. But the real seismic data in the application section, which is very large, are not available because they involve business secrets.

Conflicts of Interest

The authors declare that they have no conflicts of interest.

Acknowledgments

This study is financially supported by National Science and Technology Major Project (Grant no. 2017ZX05005-004-002) and NSFC and Sinopec Joint Key Project (U1663207). We also acknowledge Miss Jie Li for her patient editing.

References

[1] J. P. Castagna and M. M. Backus, "AVO analysis—tutorial and review," in *Offset-dependent reflectivity: theory and practice of AVO analysis: SEG investigations in geophysics*, vol. 8, pp. 3–36, Society of Exploration Geophysicists, 1993.

[2] W. J. Ostrander, "Plane-wave reflection coefficients for gas sands at nonnormal angles of incidence," *Geophysics*, vol. 49, no. 10, pp. 1637–1648, 1984.

[3] P. Avseth, T. Mukerji, A. Jørstad, G. Mavko, and T. Veggeland, "Seismic reservoir mapping from 3-D AVO in a North Sea turbidite system," *Geophysics*, vol. 66, no. 4, pp. 1157–1176, 2001.

[4] J. P. Castagna, H. W. Swan, and D. J. Foster, "Framework for AVO gradient and intercept interpretation," *Geophysics*, vol. 63, no. 3, pp. 948–956, 1998.

[5] C. C. Diaconescu, R. M. Kieckhefer, and J. H. Knapp, "Geophysical evidence for gas hydrates in the deep water of the South Caspian Basin, Azerbaijan," *Marine and Petroleum Geology*, vol. 18, no. 2, pp. 209–221, 2001.

[6] B. Pan, M. K. Sen, and H. Gu, "Joint inversion of PP and PS AVAZ data to estimate the fluid indicator in HTI medium: a case study in Western Sichuan Basin, China," *Journal of Geophysics and Engineering*, vol. 13, no. 5, pp. 690–703, 2016.

[7] A. C. B. Ramos and J. P. Castagna, "Useful approximations for converted-wave AVO," *Geophysics*, vol. 66, no. 6, pp. 1721–1734, 2001.

[8] R. Verm and F. Hilterman, "Lithology color-coded seismic sections: the calibration of AVO crossplotting to rock properties," *The Leading Edge*, vol. 14, no. 8, pp. 847–853, 1995.

[9] X. Wei, T. Chen, and Y. Ji, "Converted wave AVO inversion for average velocity ratio and shear wave reflection coefficient," *Applied Geophysics*, vol. 5, no. 1, pp. 35–43, 2008.

[10] M. A. Biot, "Theory of propagation of elastic waves in a fluid-saturated porous solid. I. Low-frequency range," *The Journal of the Acoustical Society of America*, vol. 28, no. 2, pp. 168–178, 1956.

[11] J. V. M. Borgomano, L. Pimienta, J. Fortin, and Y. Guéguen, "Dispersion and attenuation measurements of the elastic moduli of a dual-porosity limestone," *Journal of Geophysical Research: Solid Earth*, vol. 122, no. 4, pp. 2690–2711, 2017.

[12] J. M. Carcione and S. Picotti, "P-wave seismic attenuation by slow-wave diffusion: effects of inhomogeneous rock properties," *Geophysics*, vol. 71, no. 3, pp. 1–8, 2006.

[13] J. Liu, J. Ba, J. W. Ma, and H. Z. Yang, "An analysis of seismic attenuation in random porous media," *Science China Physics, Mechanics and Astronomy*, vol. 53, no. 4, pp. 628–637, 2010.

[14] A. N. Norris, "Low-frequency dispersion and attenuation in partially saturated rocks," *The Journal of the Acoustical Society of America*, vol. 94, no. 1, pp. 359–370, 1993.

[15] L. Pimienta, J. Fortin, and Y. Guéguen, "Bulk modulus dispersion and attenuation in sandstones," *Geophysics*, vol. 80, 2015.

[16] S. R. Pride, J. G. Berryman, and J. M. Harris, "Seismic attenuation due to wave-induced flow," *Journal of Geophysical Research: Solid Earth*, vol. 109, no. B1, 2004.

[17] M. Chapman, E. Liu, and X. Y. Li, "The influence of abnormally high reservoir attenuation on the AVO signature," *The Leading Edge*, vol. 24, no. 11, pp. 1120–1125, 2005.

[18] A. Wilson, M. Chapman, and X. Y. Li, "Frequency-dependent AVO inversion," in *79th annual SEG meeting Expanded Abstracts*, vol. 28, pp. 341–345, Society of Exploration Geophysicists, 2009.

[19] X. Wu, M. Chapman, A. Wilson, and X. Y. Li, "Estimating seismic dispersion from pre-stack data using frequency-dependent AVO inversion," in *SEG Technical Program Expanded Abstracts 2010*, vol. 29, pp. 425–429, Society of Exploration Geophysicists, 2010.

[20] B. J. Cheng, T. G. Xu, and S. G. Li, "Research and application of frequency dependent AVO analysis for gas recognition," *Chinese Journal of Geophysics*, vol. 55, no. 2, pp. 608–613, 2012.

[21] S. Q. Chen, X. Y. Li, and X. Y. Wu, "Application of frequency-dependent AVO inversion to hydrocarbon detection," *Journal of Seismic Exploration*, vol. 23, pp. 241–264, 2014.

[22] Y. Li, L. Zhang, D. Wang, S. Shi, and X. Cui, "Hydrocarbon detection for Ordovician carbonate reservoir using amplitude variation with offset and spectral decomposition," *Interpretation*, vol. 4, no. 3, pp. SN11–SN30, 2016.

[23] X. Y. Wu, M. Chapman, and X. Y. Li, "Estimating seismic dispersion from pre-stack data using frequency dependent AVO analysis," *Journal of Seismic Exploration*, vol. 23, pp. 219–239, 2014.

[24] K. Aki and P. G. Richards, *Quantitative Seismology*, vol. 2, W. H. Freeman, New York, 1980.

[25] G. C. Smith and P. M. Gidlow, "Weighted stacking for rock property estimation and detection of gas," *Geophysical Prospecting*, vol. 35, no. 9, pp. 993–1014, 1987.

[26] L. Cohen, *Time-Frequency Analysis*, Prentice Hall Inc., New York, USA, 1995.

[27] X. Wu, *Frequency dependent AVO inversion using spectral decomposition techniques*, China University of Geosciences, Wuhan, 2010.

[28] J. Liu, J. W. Ma, and H. Z. Yang, "Research on P-wave's propagation in White's sphere model with patchy saturation," *Chinese Journal of Geophysics-Chinese Edition*, vol. 53, no. 4, pp. 954–962, 2010.

[29] S. B. Liu, S. J. Huang, Z. M. Shen, Z. X. Lü, and R. C. Song, "Diagenetic fluid evolution and water-rock interaction model of carbonate cements in sandstone: an example from the reservoir sandstone of the fourth member of the Xujiahe formation of the Xiaoquan-Fenggu area, Sichuan Province, China," *Science China Earth Sciences*, vol. 57, no. 5, pp. 1077–1092, 2014.